WATER VAPOUR AND TEMPERATURE MEASUREMENTS BY RAMAN LIDAR IN THE FRAME OF THE NDACC

Benedetto De Rosa[1*], Paolo Di Girolamo[1], Donato Summa[1]

[1] *Scuola di Ingegneria, Università degli Studi della Basilicata, Potenza, 85100, Italy*
**Email: bundit@hotmail.it*

ABSTRACT

In November 2012, the University of BASILicata Raman Lidar system (BASIL) was approved to enter the International Network for the Detection of Atmospheric Composition Change (NDACC). Since then measurements were routinely carried out on a once per week basis. This paper illustrates specific measurement examples from this effort, with a dedicated focus on temperature and water vapour measurements, with the ultimate goal to provide a characterization of the system performance. Case studies illustrated in this paper demonstrate the ability of BASIL to perform measurements of the temperature profile up to 50 km and of the water vapour mixing ratio profile up to 15 km, based on an integration time of 2 hours and a vertical resolution of 150 m, with measurement bias not exceeding 0.1 K and 0.1 g kg^{-1}, respectively. Raman lidar measurements are compared with measurements from additional instruments, such as radiosondings and satellite sensors (IASI and AIRS), and with model re-analyses data (ECMWF and ECMWF-ERA). Comparisons in this paper cover the altitude interval up to 15 km for water vapour mixing ratio and up to 50 km for the temperature. Comparisons between BASIL and the different sensor/model data in terms of water vapour mixing ratio indicate a mean absolute/relative bias of -0.024 g kg^{-1}(or -3.9 %), 0.342 g kg^{-1}(or 36.8 %), 0.346 g kg^{-1} (or 37.5 %), -0.297 g kg^{-1} (or -25 %), -0.381 g kg^{-1} (or -31 %), when compared with radisondings, AIRS, IASI, ECMWF, ECMWF-ERA, respectively. For what concerns the comparisons in terms of temperature measurements, these indicate a mean absolute bias between BASIL and the radisondings, AIRS, IASI, ECMWF, ECMWF-ERA of -0.04, 1.99, 0.48, 0.14, 0.62 K, respectively. Based on the available dataset and benefiting from the circumstance that the Raman lidar BASIL could be compared with all other sensor/model data, it has been possible to estimate the absolute bias of all sensors/datasets, this being 0.004 g kg^{-1}/0.30 K, 0.021 g kg^{-1}/-0.34 K, -0.35 g kg^{-1}/0.18 K, -0.346 g kg^{-1}/-1.63 K, 0.293 g kg^{-1}/-0.16 K and 0.377 g kg^{-1}/0.32 K in terms of water vapour mixing ratio/temperature for BASIL, the radisondings, IASI, AIRS, ECMWF, ECMWF-ERA, respectively.

1. INTRODUCTION

Water vapour is the most important atmospheric greenhouse gas and its increasing concentration, though indirectly, is primarily driven by human activity. The increasing concentration of CO_2 and CH_4, primarily associated with fossil fuel combustion, leads to warmer tropospheric temperatures, which determine an increased atmospheric humidity content and ultimately lead to a warmer climate. Moreover, water vapour in the upper troposphere/lower stratosphere (UTLS) region plays a crucial role in the Earth radiative balance, and consequently in the climate system, its presence being primarily associated with two main sources: transport from the troposphere, taking place mainly in the tropics, and the in-situ oxidation of methane. More specifically, changes in temperature and water vapour concentration in the UTLS result in radiative forcing alterations [1], which trigger climate changes (Intergovernmental Panel on Climate Change, 2007). Observations demonstrate that stratospheric water vapour increases with increasing tropospheric temperature, implying the existence of a stratospheric water vapour feedback [2]. The strength of this feedback has been estimated to be ~ 0.3 W m^{-2} K^{-1}. Stratospheric water vapour has also an important role in stratospheric clouds formation, which are a key element in stratospheric ozone depletion mechanisms [3, 4]. Furthermore, stratospheric water vapour is important in the formation of hydrogen radicals, which play a role in stratospheric chemistry and stratospheric ozone depletion. Despite the major importance of having accurate water vapour and temperature measurements in the troposphere and stratosphere, few measurements of these variables and of their long-term variability are available,

especially in the UTLS region. Water vapour, measurements in the UTLS region have been traditionally guaranteed by the use of operational radiosondes or balloon-borne frost-point hygrometers, the latter sensor remaining the best source of high quality water vapour measurements in this region. However, these are too expensive to be used on an operational basis and thus do not allow a sufficiently intense launch schedule to guarantee the high temporal resolution needed for the above mentioned scientific scopes. Similar considerations apply to temperature, the main source of measurements covering the troposphere and stratosphere being represented by microwave and infrared satellite sounders. All the above weather and climate-related issues call for highly accurate measurements of both the water vapour and temperature profiles throughout the atmosphere, with a specific focus on the UTLS region. These motivations pushed the international Network for the Detection of Stratospheric Change (NCSC), now Network for the Detection of Atmospheric Composition Change (NDACC), to include in the early 2000s water vapour Raman lidars and temperature lidars among its instruments.

2. METHODOLOGY

2.1 The lidar system

The Raman Lidar system BASIL joined NDACC in November 2012, with the primary goal of providing accurate routine measurements of the vertical profiles of both water vapour mixing ratio and temperature. The setup of BASIL has been described in a variety of previous papers [5-7]. A mobile version of the system has been deployed in several international field campaigns [8-18]. BASIL measurements of the temperature profile cover the full altitude interval from the surface up to the stratopause. Measurements over such a wide altitude interval are possible based on the combined application of the pure rotational Raman technique [19, 20] which is used to cover the lowest 20 km, and the integration technique, covering the altitude region from 20 km to typically 50-55 km. The combined application of these two techniques is possible because of the presence of an overlap region (20-25 km) where both techniques properly work. Recently, the aerosol backscattering coefficient at 354.7 nm has been added to the set of atmospheric variables measured by BASIL and uploaded to NDACC repository.

3. RESULTS

3.1 Measurements

For the purpose of this paper, we focused our attention on four selected case studies collected during the first 2 years of operation of the system, namely 7 November 2013, 9 October 2014 and 2 and 9 April 2015. While a larger data-set could have been chosen, we decided to focus our attention to a limited number of case studies, which have been carefully analyzed with a customized approach, instead of considering a larger dataset analyzed with a standard routine analysis approach. This approach was considered with the aim of minimizing the effects associated with the application of the data analysis approach. The four selected case studies cover a two year time interval from the early stage of BASIL operation in the frame of NDACC (7 November 2013 to April 2015). Figure 1a illustrates the mean water vapour mixing ratio profile measured by BASIL on 9 October 2014 over the time interval 16:00-18:00 UTC, together with the closest in time vertical profiles the water vapour mixing ratio profiles from IASI (at 19:20 UTC) and AIRS (at 14:35 UTC) and the model re-analysis ECMWF ERA-15 and ECMWF ERA-40 (at 18:00 UTC). The vertical resolution of the Raman lidar data is 150 m up to 6 km, 300 m between 6 and 8 km and 600 m above 8 km, with the water vapour mixing ratio profile extending up to an altitude of ~ 14 km, with values down to 0.02 g kg^{-1}. Similar performances are found in all two-hour profiles collected in the frame of NDACC. The present comparison also includes the radiosonde profile launched at 18:00 UTC from the nearby station IMAA-CNR (~ 7 km W). Deviations between BASIL and the radiosonde are not exceeding 0.1 g kg^{-1} up to ~ 9 km. Figure 1b illustrates the mean atmospheric temperature profile measured by BASIL over the same time interval considered in figure 1a, together with the corresponding profiles from IASI, AIRS and the model re-analysis (ECMWF ERA-15 and ECMWF ERA-40). The lidar measurement is based on the use of the rotational technique up to 20 km and the integration technique above 20 km.

The deviations observed above 35 km are possibly associated with the effects of gravity waves propagation, whose presence is revealed by the Raman lidar, but missed by the other sensors/models. The temperature profile from the radiosonde extends up to 30 km. Water vapour mixing ratio and temperature deviations between BASIL and the radiosonde are smaller than those characterizing any other sensors/models pair.

3.1 Mean Bias

The performance of the different profiling sensors and models considered in the study are assessed through a statistical analysis. Figures 2a and b illustrate the water vapour mixing ratio absolute and percentage BIAS for all sensor/model pairs. As expected, the absolute BIAS shows larger values in the ABL (in the range -3/+5 g kg^{-1}), with values being typically smaller than ±1 g kg^{-1} above 2 km. More specifically, in the ABL the absolute BIAS of BASIL vs. the radiosondes is in the range ±0.3 g kg^{-1}.For all sensor/model pairs, the absolute BIAS shows values smaller than ±0.1 g kg^{-1} above 8 km and smaller than ±0.02 g kg^{-1} above 10 km. In the altitude region 8-16 km the mutual bias of BASIL vs. the radiosondes or ECMWF is smaller than ±0.01 g kg^{-1}, while the mutual bias of BASIL vs. ECMWF-ERA40 and AIRS vs. IASI is smaller than ±0.07 g kg^{-1} above 10 km. For all sensor/model pairs, the relative or percentage BIAS shows values in the range ±60 % all the way up to 16 km. The smallest percentage bias values are found in the comparison of BASIL vs. the radiosondes, with values not exceeding ±18 % all the way up to 12 km and values in the range ±13 % above the ABL up to 4 km. Small percentage bias values are also found in the comparison of BASIL vs. ECMWF, with values not exceeding ±30 %. Figure 2c illustrates the temperature absolute BIAS profiles for all sensor/model pairs. The BIAS of BASIL vs. the radiosondes is in the range ±1 K above the ABL up to 12 km, with deviations in the ABL not exceeding 2 K. With the exception of a few data points, BIAS values are within ±2 K up to 30 km, which is the maximum altitude reached by the radiosonde. The BIAS of BASIL vs. ECMWF-ERA40 is in the range ±0.8 K up to 12.5 km. For all sensor/model pairs, the BIAS shows values in the range ±5 K all the way up to 50 km.

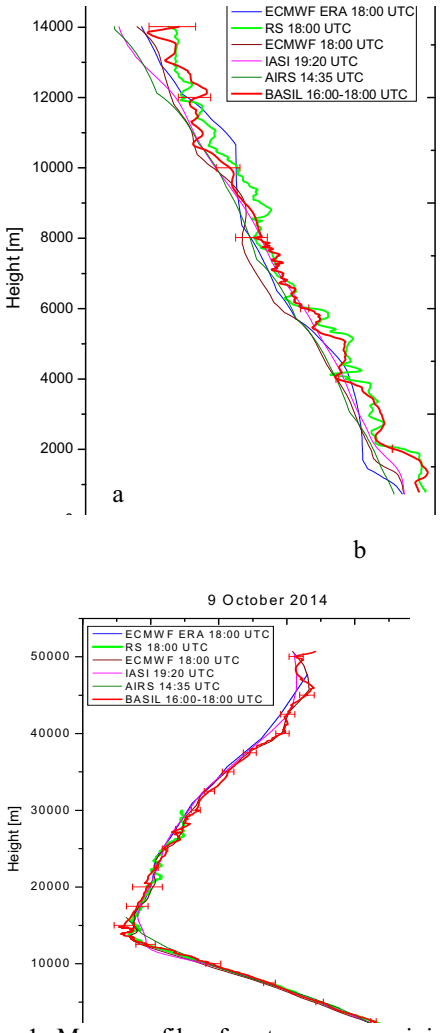

Fig. 1: Mean profile of water vapour mixing ratio (a) and temperature (b) as measured by BASIL over the time interval 16:00-18:00 UTC on 9 October 2014, together with the closest in time profiles from IASI (at 19:20 UTC), AIRS (at 14:35 UTC) and the model re-analysis ECMWF (ERA-15 & ERA-40, at 18:00 UTC).

RMS deviation values for both water vapour mixing ratio and temperature for all sensor/model pairs (not shown here) are slightly larger than BIAS values, which testifies the limited contribution of statistical uncertainties and geophysical changes in the deviations between the different measured/modeled profile pairs. The vertically-averaged mean bias over the whole inter-comparison range is obtained through the application of a weighted mean. Results from the present inter-comparison effort provide evidence of the high quality of water vapour and temperature profile measurements from BASIL and on the possibility to use these measurements

for the long-term monitoring of atmospheric composition and thermal structure changes.

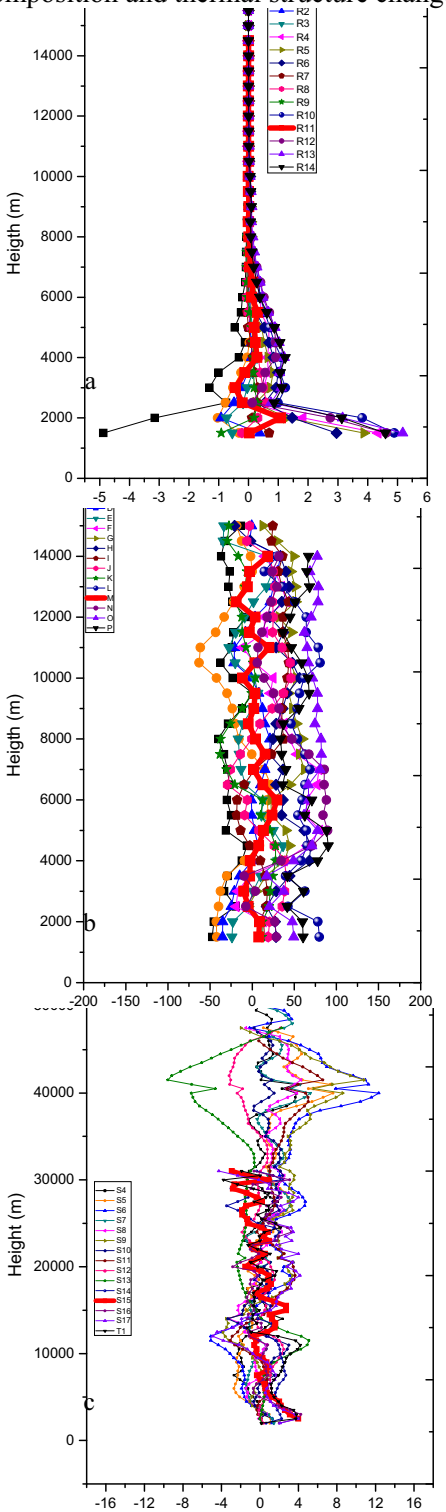

Fig 8: Vertical profiles of water vapour mixing ratio mean absolute BIAS (a) percentage BIAS (b) and vertical profiles of temperature mean absolute BIAS (c).

REFERENCES

[1] M. Riese, et al. Geophys. Res. 117, D16305, doi: 10.1029/2012JD017751 (2012).
[2] A. Dessler, et al. Natl. Acad. Sci. USA 110, 18087-18091, doi: 10.1073/pnas.1310344110 (2013).
[3] A. Di Sarra, et al. Geophys. Res. Lett. 19, 1823-1826, doi: 10.1029/92GL01887 (1992).
[4] P. Di Girolamo, et al. Geophys. Res. Lett. 21, 1295-1298, doi: 10.1029/93GL02892 (1994).
[5] P. Di Girolamo, et al. Multiparameter Raman Lidar Measurements for the Characterization of a Dry Stratospheric Intrusion Event, J. Atmos. Oceanic Technol. 26, 1742-1762, doi: 10.1175/2009JTECHA1253.1 (2009).
[6] P. Di Girolamo, et al., UV Raman lidar measurements of relative humidity for the characterization of cirrus cloud microphysical properties, Atmos. Chem. Phys. 9, 8799-8811, doi: 10.5194/acp-9-8799-2009 (2009).
[7] R. Bhawar, et al. Q. J. Roy. Meteor. Soc. 137, 325-348, doi: 10.1002/qj.697 (2011).
[8] R. Bhawar, et al. Geophysical Research Letters 35, L04812, doi: 10.1029/2007GL032207 (2008).
[9] C. Serio, et al. Optics Express 16/20, 15816-15833 doi: 10.1364/OE.16.015816 (2008).
[10] V. Wulfmeyer, et al. Bulletin of the American Meteorological Society 89, 1477-1486, doi: 10.1175/2008BAMS2367.1 (2008).
[11] L. J. Bennett et al., Q. J. Roy. Meteor. Soc. 137, 176-189, doi: 10.1002/qj.760 (2011).
[12] V. Ducrocq, et al. Bull. Amer. Meteor. Soc. 95, 1083-1100, doi: 10.1175/BAMS-D-12-00244.1 (2014).
[13] A. Macke, et al. Atmos. Chem. Phys. 17, 4887-4914, doi:10.5194/acp-17-4887-2017 (2017).
[14] Di Girolamo, et al. Atmos. Environ. 50, 66-78, 10.1016/j.atmosenv.2011.12.061 (2012).
[15] P. Di Girolamo, et al. Atmos. Chem. Phys. 12, 4143-4157, doi: 10.5194/acp-12-4143-2012 (2012).
[16] P. Di Girolamo, et al. Q. J. Roy. Meteor. Soc., 142, 153-172, doi: 10.1002/qj.2767 (2016).
[17] P. Di Girolamo, et al., Characterisation of Boundary Layer Turbulent Processes by the Raman lidar BASIL In the frame of HD(CP)2 Observational Prototype Experiment, Atmos. Chem. Phys., 17, 745-767, doi:10.5194/acp-17-745-2017 (2017).
[18] P. Di Girolamo, et al. Atmos. Chem. Phys., 18, 4885-4896, doi: 10.5194/acp-18-4885-2018 (2018).
[19] A. Behrendt and J. Reichardt, Appl. Opt. 39, 1372–1378, doi: 10.1364/AO.39.001372 (2000).
[20] P. Di Girolamo, et al., Rotational Raman Lidar measurements of atmospheric temperature in the UV, Geophys. Res. Lett. 31, doi: 10.1029/2003GL018342 (2004).